

1N-27
139955
P.18

Kinetics of Hexacelsian to Celsian Phase Transformation in $\text{SrAl}_2\text{Si}_2\text{O}_8$

Narottam P. Bansal
Lewis Research Center
Cleveland, Ohio

and

Charles H. Drummond, III
Ohio State University
Columbus, Ohio

Prepared for the
94th Annual Meeting of the American Ceramic Society
sponsored by the American Ceramic Society
Minneapolis, Minnesota, April 12-16, 1992



(NASA-TM-105913) KINETICS OF
HEXACELSIAN TO CELSIAN PHASE
TRANSFORMATION IN $\text{SrAl}_2\text{Si}_2\text{O}_8$
(NASA) 18 p

N93-16372

Unclass

63/27 0139888

480621

KINETICS OF HEXACELSIAN TO CELSIAN PHASE TRANSFORMATION IN $\text{SrAl}_2\text{Si}_2\text{O}_8$

NAROTTAM P. BANSAL

National Aeronautics and Space Administration
Lewis Research Center
Cleveland, Ohio 44135

and

CHARLES H. DRUMMOND, III*

Department of Materials Science and Engineering
The Ohio State University
Columbus, Ohio 43210

ABSTRACT

The kinetics of hexacelsian to celsian phase transformation in $\text{SrAl}_2\text{Si}_2\text{O}_8$ have been investigated. Phase pure hexacelsian was prepared by heat treatment of glass flakes at 990 °C for 10 h. Bulk hexacelsian was isothermally heat treated at 1026, 1050, 1100, 1152, and 1200 °C for various times. The amounts of monoclinic celsian formed were determined using quantitative X-ray diffraction. Values of reaction rate constant, k , at various temperatures were evaluated from the Avrami equation. The Avrami parameter was determined to be 1.1, suggesting a diffusionless, one-dimensional transformation mechanism. From the temperature dependence of k , the activation energy for this reaction was evaluated to be 527 ± 50 kJ/mole (126 ± 12 kcal/mole). This value is consistent with a mechanism involving the transformation of the layered hexacelsian structure to a three-dimensional network celsian structure which necessitates breaking of the strongest bonds, the Si-O bonds.

*Summer Faculty Fellow at NASA Lewis Research Center.

INTRODUCTION

Strontium aluminosilicate glass of $\text{SrAl}_2\text{Si}_2\text{O}_8$ (SAS) composition is being investigated^{1,2} for fiber-reinforced glass-ceramic matrix composites for high temperature structural applications in aerospace propulsion and power systems. When SAS glass is heat treated, both hexacelsian and monoclinic celsian phases having the composition $\text{SrAl}_2\text{Si}_2\text{O}_8$ crystallize. Celsian is the stable phase below its melting point ($\sim 1650^\circ\text{C}$) and does not exhibit any phase transformation. It also has a low thermal expansion and is one of the most refractory glass-ceramic compositions. In contrast, hexacelsian is a metastable phase and undergoes reversible structural transformations at $\sim 600^\circ\text{C}$ and $\sim 760^\circ\text{C}$, accompanied by volume changes. In the presence of fibers, these volume changes lead to undesirable residual stresses and possible matrix cracking. The hexacelsian phase should thus be avoided in the matrix material of fiber-reinforced $\text{SrAl}_2\text{Si}_2\text{O}_8$ composites.

The objective of the present investigation was to study the time-temperature kinetics of hexacelsian to celsian phase transformation in $\text{SrAl}_2\text{Si}_2\text{O}_8$. Rate constants for this reaction were determined at various temperatures between 1025 and 1200°C using the Avrami equation, and the activation energy was evaluated from the temperature dependence of the rate constant.

EXPERIMENTAL METHODS

Glass of stoichiometric composition, $\text{SrAl}_2\text{Si}_2\text{O}_8$, was melted at

~2000 °C in a continuous electric melter with Mo electrodes using laboratory grade SrCO_3 , Al_2O_3 , and SiO_2 . Homogeneous and clear glass flakes were produced by quenching the melt between water-cooled metallic rollers. From wet chemical analysis, the as-melted glass composition (weight %) was determined to be 33.7 SrO, 31.5 Al_2O_3 , 33.8 SiO_2 , 0.12 Na_2O , 0.86 BaO, and 0.01 MoO_3 . The Mo was estimated by a spectrographic technique. The batch composition in weight percent was 31.8 SrO, 31.3 Al_2O_3 , and 36.9 SiO_2 which corresponds to the celsian formula.

Isothermal heat treatments of the glass flakes were carried out in a programmable Lindberg box furnace, with temperature control of better than ± 5 °C of the set value. The flakes were air-quenched and ground to pass through a 325 mesh sieve. Powder X-ray diffraction (XRD) patterns were recorded using a step scan procedure ($0.03^\circ/2\theta$ step, count time 0.5 s) on a Philips ADP-3600 automated powder diffractometer equipped with a crystal monochromator and employing copper K_α radiation.

Hexacelsian was synthesized by heat treatment of glass flakes at 990 °C for 10 h in air. Single phase monoclinic celsian was prepared from SAS glass powder by isothermal heat treatment at 1300 °C for 10 h in air. Reference standards of various compositions were prepared by mixing hexacelsian and celsian in different weight ratios. The area under two monoclinic XRD peaks ($2\theta = 27.2$ and 27.6°), which did not overlap with the hexacelsian peaks, was measured and a calibration curve of peak area vs. weight % celsian was established. The weight fraction of celsian was determined in

isothermally heat-treated hexacelsian flakes at temperatures between 1025 and 1200 °C for times ranging from 5 min to 100 h. XRD scans were run in triplicate for standard and the heat-treated samples.

Optical microscopy was carried out on fracture surfaces of bulk specimens, ground and polished to 0.5 μ m, and etched for 5 - 10 sec with a solution consisting of 1HF + 2HNO₃ + 97H₂O (parts by volume).

RESULTS

Powder XRD patterns of hexacelsian and celsian prepared by controlled heat treatments of SAS glass are compared in Fig. 1. From XRD, both the materials are phase pure. The doublet at $2\theta = 27.2$ and 27.6° is the strongest diffraction peak for celsian and has no interference from hexacelsian. The area under this doublet was, therefore, measured to monitor the progress of hexacelsian to celsian conversion on isothermal heat treatments at various temperatures. Powder XRD patterns of standard mixtures of various compositions are presented in Fig. 2. Intensity of the doublet increased linearly with the amount of celsian in the mixture as shown by the X-ray calibration curve (Fig. 3), in the form of peak area in counts vs. weight % celsian. Data from triplicate runs for each standard mixture are shown. The solid line, obtained from linear regression analysis, had a slope of 6.939 and an intercept of 22.2. The correlation coefficient was 0.9856 indicating an excellent fit of the data. The small positive intercept may indicate the presence of a trace amount of celsian in the starting

hexacelsian material. The amount of celsian in an unknown sample can then be determined from the equation:

$$\text{Weight \% celsian} = [\text{Peak area} - 22.2]/6.939$$

where "peak area" is the area under the XRD doublet.

Figure 4 shows the powder XRD patterns of hexacelsian flakes heat treated at 1100 °C for various times. The celsian phase was detected in the 0.5 h sample; its concentration increased with time of heat treatment. The hexacelsian phase was almost completely absent in the 30 h specimen. Powder X-ray diffractograms of bulk hexacelsian heat treated for 2 h at various temperatures are compared in Fig. 5. The 1152 °C sample shown here was heated for only 1 h. Celsian was just detected in the 1026 °C heat treated sample. At higher temperatures, more and more celsian was formed and at 1200 °C, the hexacelsian was fully transformed to celsian.

Optical micrographs of polished and etched surfaces of hexacelsian flakes heat treated at 1100 °C for various times are shown in Fig. 6. Elongated grains of hexacelsian growing inward from the surface are present. The band in the middle is probably where the hexacelsian grains growing from the two opposite edges met. Celsian appears to nucleate at the surface and grows inward. The celsian phase probably also nucleates at the interface of hexacelsian crystals in the bulk.

The Avrami equation, which is a good description³ for a phase change by a nucleation and growth process, was used to evaluate the

reaction rate constant at each temperature:

$$x = 1 - \exp[-(kt)^n] \quad (1)$$

where x is the volume fraction transformed after time t , k is the reaction rate constant, and n is the Avrami exponent which is related to the mechanism of crystal growth. Rearranging eq.(1) and taking logarithms gives

$$\ln[-\ln(1-x)] = n \ln k + n \ln t \quad (2)$$

according to which a plot of $\ln[-\ln(1-x)]$ vs. $\ln t$ should be linear with a slope of n and intercept $n \ln k$. The Avrami plots for hexacelsian to celsian transformation in bulk SAS at 1026, 1050, 1100, 1152, and 1200 °C are shown in Fig. 7. The solid lines are obtained from linear regression analysis of the data. Values of k and n at each temperature are listed in Table I. The rate constant increased sharply with temperature -- by more than two orders of magnitude as the temperature was raised from 1026 to 1200 °C.

Temperature dependence of k is expressed by the Arrhenius equation:

$$k = \nu \exp[-E/RT] \quad (3)$$

where ν is the attempt frequency, E the transformation activation energy, R the gas constant, and T the isothermal reaction tempera-

ture in Kelvin. An Arrhenius plot of $\ln k$ vs. $1/T$ for the data of Table I is presented in Fig. 8. A linear regression analysis of the data resulted in a value of 527 ± 50 kJ/mole (126 ± 12 kcal/mole) for E and $\nu = 4.3 \times 10^{15}/s$, with a correlation coefficient of -0.999 , indicating an excellent fit.

DISCUSSION

Our value of activation energy for hexacelsian to celsian transformation in SAS is compared with the literature⁴ value for the $BaAl_2Si_2O_8$ (BAS) system in Table II. A value of 527 kJ/mole in the present study for the SAS system is larger than the Si-O and Al-O single bond strengths. A value of 84 kJ/mole for a similar transformation in the BAS system, obtained by Bahat⁴ using an infrared spectroscopic technique, is too low and not consistent with the hexacelsian to celsian transformation mechanism. We believe Bahat's analysis of his data is in error. In Fig. 4 of Bahat's paper⁴, which shows plots of weight % hexacelsian vs. time of heat treatment at various temperatures, an extrapolation to zero time does not result in zero per cent transformation. Furthermore, these extrapolated values at $t = 0$ were erroneously taken⁴ as the reaction rate constants k at various temperatures. We have recently reanalyzed Bahat's data using the Avrami equation (1), and an activation energy of 373 kJ/mole (89 kcal/mole) was obtained⁵ for hexacelsian to celsian transformation in $BaAl_2Si_2O_8$. This recalculated value of E is much greater than 84 ± 17 kJ/mole reported by

Bahat⁴.

The crystal structure of hexacelsian⁶ (Fig. 9A) contains infinite two-dimensional hexagonal sheets consisting of two layers of (Al,Si)O₄ tetrahedra. These tetrahedra share three corners with the remaining apices pointing in the same direction. Two of these sheets share their apical oxygens, forming a double tetrahedral sheet. Sr ions compensate for the charge difference between Al and Si and occupy positions between the double sheets with twelve equidistant oxygen neighbors. Celsian consists of a three-dimensional feldspar structure⁷ (Fig. 9B) in which all four vertices of the silica tetrahedra are shared forming a three-dimensional network. As in hexacelsian, Al substitutes for Si so that each Al tetrahedron is surrounded by four predominantly Si tetrahedra and vice versa. Charge compensation is by Sr ions present in the larger interstices of the framework structure. The Sr ions have an irregular configuration with ten oxygen neighbors at several Sr-O distances. Consequently, the transformation of hexacelsian to celsian would require the creation of a three-dimensional network from the two-dimensional sheet structure as well as rearrangement of the Sr sites. This must entail breaking and reforming of the Al-O and Si-O bonds.

The single bond strength⁸ of the Si-O bond is 445 kJ/mole and that of the Al-O bond with an Al coordination number of four is 330 - 423 kJ/mole. An activation energy of 527 kJ/mole for the hexacelsian to celsian transformation in SAS is consistent with the mechanism requiring the breaking of the Si-O and Al-O bonds. The

recalculated⁵ value of 373 kJ/mole for BAS is in better agreement with this mechanism than the value reported by Bahat⁴.

Celsian nuclei may have already been formed in the starting hexacelsian material (*vide supra* Fig. 3) used in this study. If this is the case or if nucleation is rapid, the measured activation energy is most likely for crystal growth, rather than for nucleation, of celsian. Since no compositional change occurs during the hexacelsian to celsian phase change, a value of unity for the Avrami parameter probably indicates³ one dimensional growth with interfacial rather than diffusion control. These conclusions are further supported by the optical micrographs in Fig. 6 which show one-dimensional growth of celsian from hexacelsian.

SUMMARY

A quantitative X-ray diffraction method has been successfully used to study the kinetics of hexacelsian to celsian transformation in $\text{SrAl}_2\text{Si}_2\text{O}_8$. The reaction rate constant for the transformation increased sharply with temperature. The activation energy for this phase change in bulk $\text{SrAl}_2\text{Si}_2\text{O}_8$ was evaluated to be 527 ± 50 kJ/mole (126 ± 12 kcal/mole), which is consistent with a mechanism involving breaking of the Al-O and Si-O bonds. The Avrami parameter was determined to be close to one, suggesting a microstructurally consistent one-dimensional, diffusionless transformation. Celsian nucleated at the surface and probably also in the bulk at the interface of hexacelsian crystals.

CONCLUSIONS

The rate of the hexacelsian to celsian transformation in $\text{SrAl}_2\text{Si}_2\text{O}_8$ (SAS) is such that it is feasible to synthesize single phase monoclinic celsian over a wide temperature range. The celsian formation would then avoid the detrimental volume changes associated with hexacelsian. Thus, SAS appears to be a suitable matrix material for fabrication of fiber-reinforced composites for high temperature structural applications.

ACKNOWLEDGMENTS

The technical assistance of John Setlock, Tom Sabo, and Ralph Garlick of NASA Lewis Research Center is gratefully acknowledged. One of us (C.H.D.) was a NASA/ASEE Summer Faculty Fellow at NASA-Lewis Research Center during the course of this research.

REFERENCES

1. C. H. Drummond, III, and N. P. Bansal, "Phase Transformations in $\text{SrAl}_2\text{Si}_2\text{O}_8$," in Proc. XVI Int'l Congress on Glass, Madrid, Spain, October 4-9, 1992; NASA TM 105657.
2. N. P. Bansal, M. J. Hyatt, and C. H. Drummond, III, "Crystallization and Properties of Sr-Ba Aluminosilicate Glass-Ceramic Matrices," *Ceram. Eng. Sci. Proc.*, **12** [7-8] 1222-34 (1991).
3. R. H. Doremus, *Rates of Phase Transformations*, Academic Press, New York, 1985, p. 26.
4. D. Bahat, "Kinetic Study on the Hexacelsian-Celsian Phase Transformation," *J. Mater. Sci.*, **5**, 805-810 (1970).
5. N. P. Bansal and C. H. Drummond, III, "Comments on Kinetic Study on the Hexacelsian-Celsian Phase Transformation," *J. Mater. Sci.*, submitted.
6. B. Yoshiki and K. Matsumoto, "High-Temperature Modification of Barium Feldspar," *J. Am. Ceram. Soc.*, **34**, 283-286 (1951).
7. R. E. Newnham and H. D. Megaw, "The Crystal Structure of Celsian (Barium Feldspar)," *Acta Cryst.*, **13**, 303-312 (1960).
8. W. D. Kingery, H. K. Bowen, and D. R. Uhlmann, *Introduction to Ceramics*, Second Edition, John Wiley, New York, 1976, p. 99.

Table I. Values of Reaction Rate Constant, k , and Avrami Parameter, n , for Hexacelsian to Celsian Transformation in Bulk $\text{SrAl}_2\text{Si}_2\text{O}_8$ at Various Temperatures

Temperature, °C	$k \times 10^6, \text{s}^{-1}$	n
1026	2.55	1.28
1050	6.41	0.94
1100	38.4	0.94
1152	220	1.13
1200	729	1.42

Table II. Values of Activation energy, E, for Hexacelsian to Celsian Phase Transformation

System	Sample form	E, kJ/mol	Technique	Reference
$\text{SrAl}_2\text{Si}_2\text{O}_8$	Bulk	527 (\pm 50)	XRD	This work
$\text{BaAl}_2\text{Si}_2\text{O}_8$	Powder	84 (\pm 17) 373	I.R.	Bahat ⁴ Ref. 5

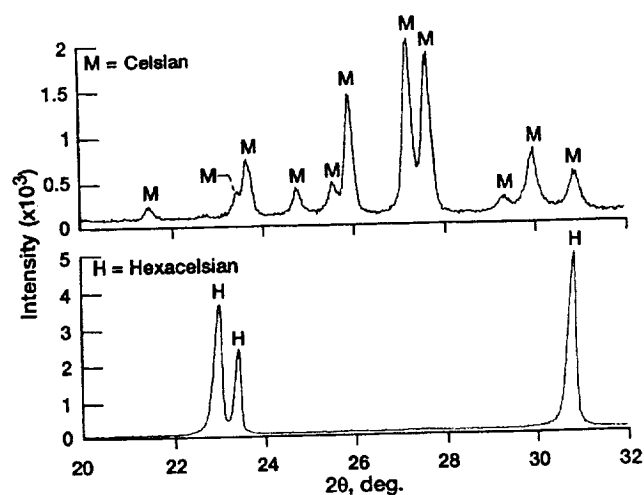


Figure 1.—Powder x-ray diffraction patterns of $\text{SrAl}_2\text{Si}_2\text{O}_8$ glass flakes heat treated at 990 °C for 10 h and glass powder at 1300 °C for 10 h.

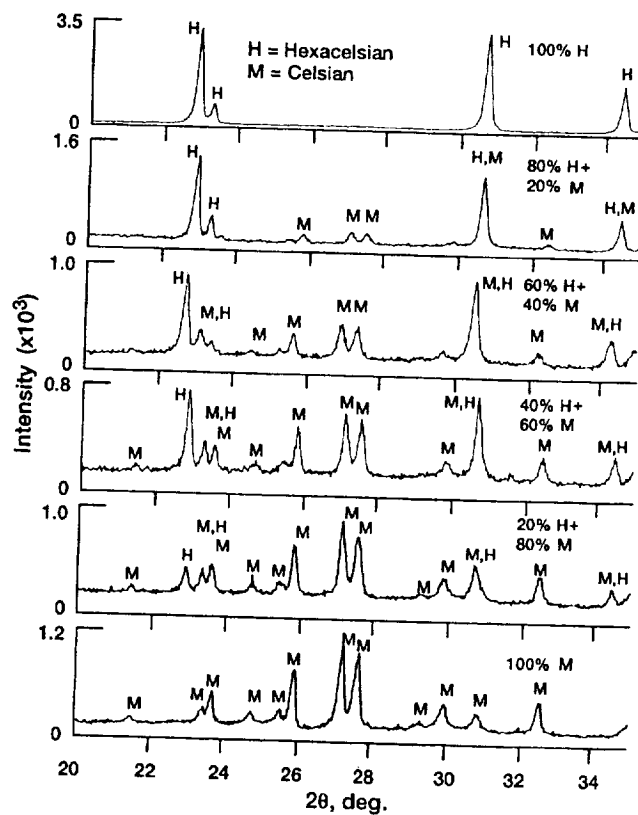


Figure 2.—Powder x-ray diffractograms of standard mixtures containing various weight percent of hexacelsian (H) and celsian (M) $\text{SrAl}_2\text{Si}_2\text{O}_8$.

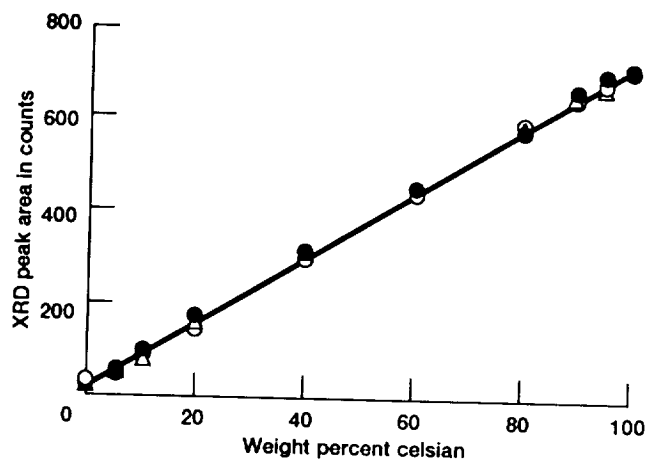


Figure 3.—XRD calibration curve for hexacelsian to celsian conversion for $\text{SrAl}_2\text{Si}_2\text{O}_8$.

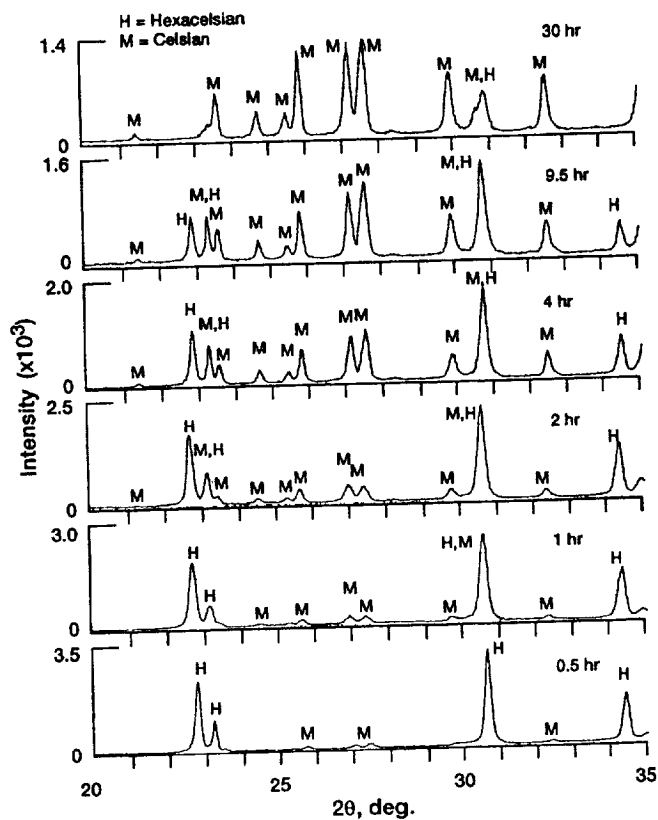


Figure 4.—Powder x-ray diffraction spectra of bulk hexacelsian $\text{SrAl}_2\text{Si}_2\text{O}_8$ heat treated at 1100°C for various times.

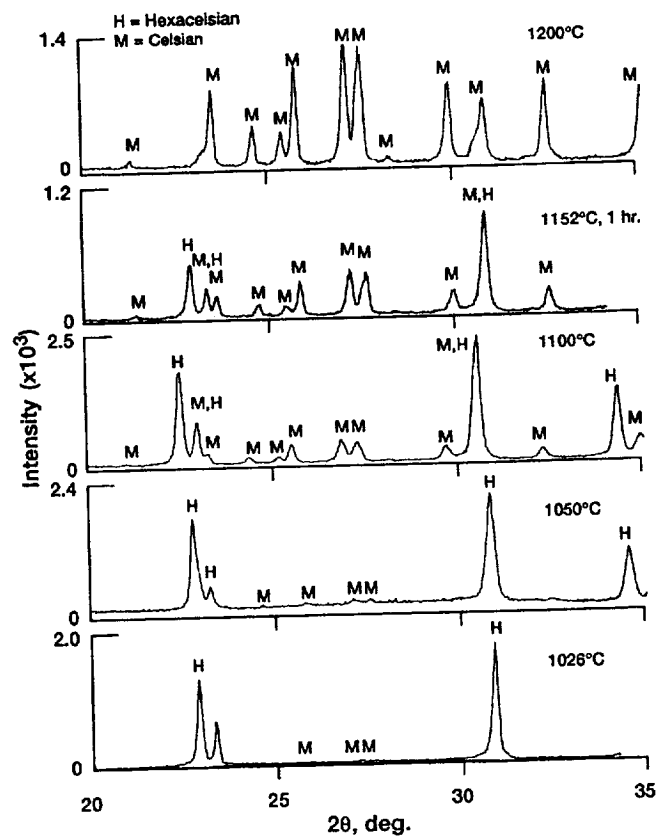


Figure 5.—Powder x-ray diffraction patterns of bulk hexacelsian $\text{SrAl}_2\text{Si}_2\text{O}_8$ heat treated for 2 h at various temperatures except for the 1152°C sample which was heated for only 1 h.

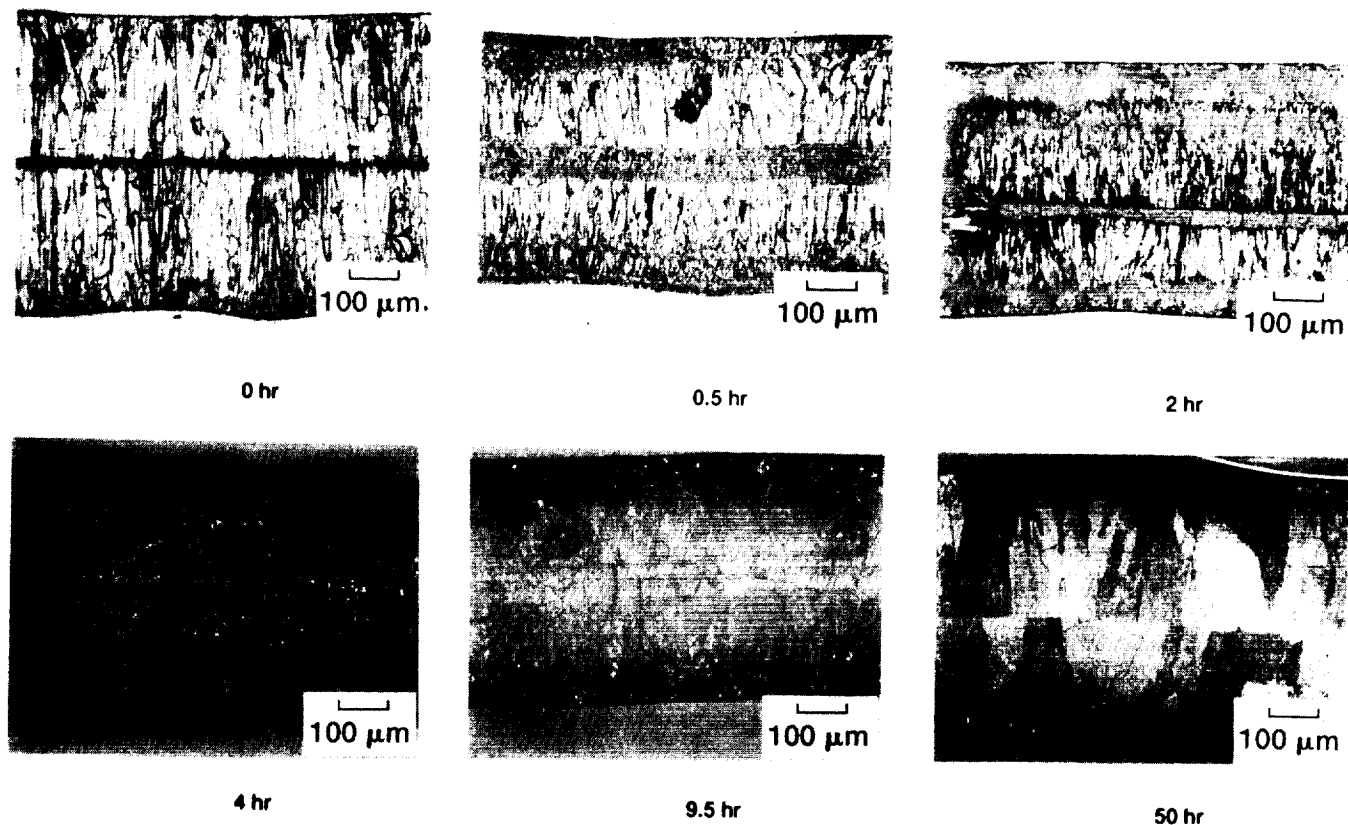


Figure 6.—Optical micrographs of polished and etched surfaces of hexacelsian $\text{SrAl}_2\text{Si}_2\text{O}_8$ flakes heat treated at 1100 °C for various times.

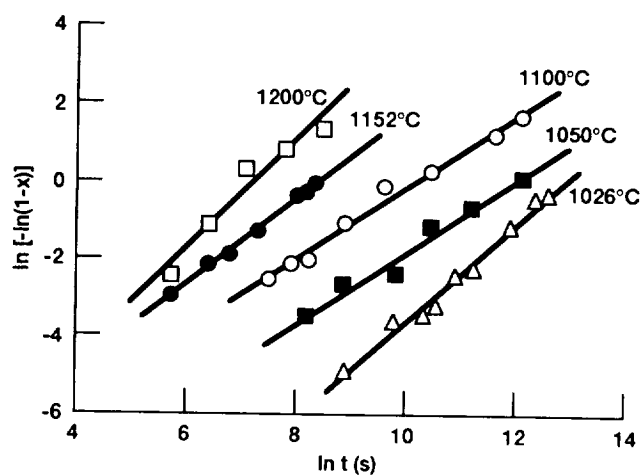


Figure 7.—Avrami plots for hexacelsian to celsian phase transformation in bulk $\text{SrAl}_2\text{Si}_2\text{O}_8$ at various temperatures.

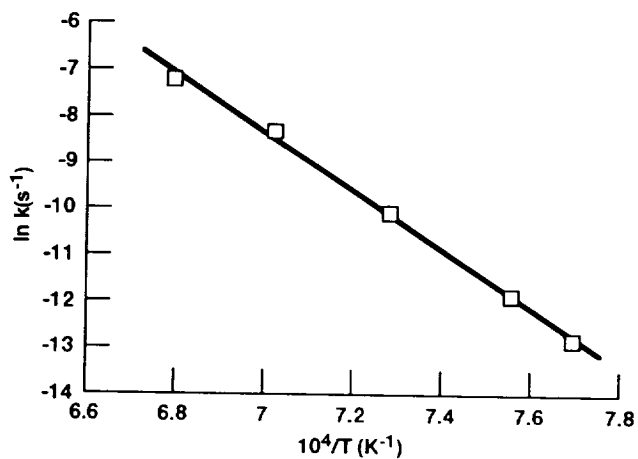


Figure 8.—Temperature dependence of reaction rate constant for hexacelsian to celsian phase transformation in bulk $\text{SrAl}_2\text{Si}_2\text{O}_8$.

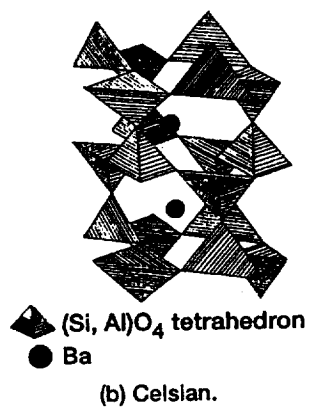
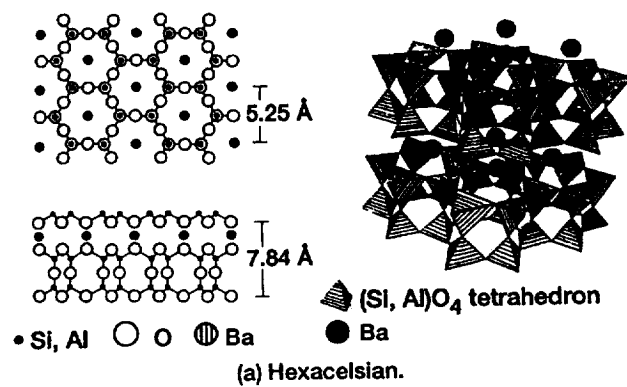


Figure 9.—Two-dimensional sheet structure of hexacelsian and three-dimensional network structure of celsian for $\text{SrAl}_2\text{Si}_2\text{O}_8$. Adopted from ref. 6 and 7.